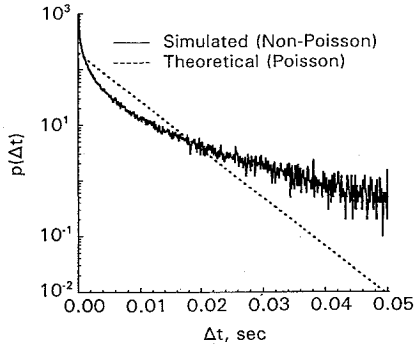

Fig. 2 Probability density function of interarrival times for simulated data, ν = 200 samples/s.

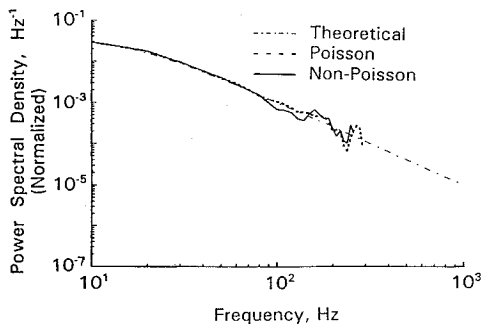

Fig. 3 Power spectra of Poisson and non-Poisson simulated data, ν = 200 samples/s.

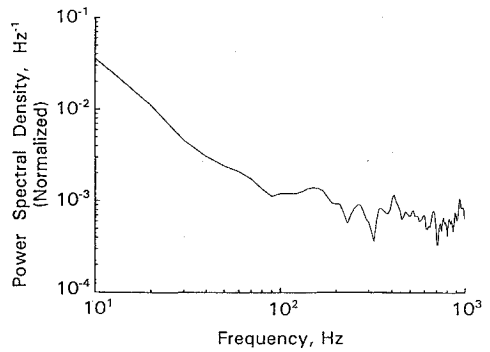

Fig. 4 Power spectrum for LV data referred to in Fig. 1, ν = 282 samples/s.

simulates the non-Poisson samples of the LV data encountered in the present study (see Fig. 1).

Results and Discussion

Power spectral density (PSD) estimates were computed using the slot-correlation technique described in Refs. 1, 2, and 4. Figure 3 shows the PSD estimates (normalized with respect to the signal variance) of the simulated first-order spectrum for both Poisson and non-Poisson sampling cases. The theoretical spectrum is also shown for comparison. The spectral estimates from the Poisson distributed samples follow the theoretical distribution up to about a frequency of 130 Hz. But in the case of non-Poisson distribution, the spectrum starts deviating from the true spectrum at a much lower frequency of about 80 Hz. The spectrum did not improve further even with larger data sets. Also, prefiltering techniques, which are normally applied to improve or extend the frequency range of the spectral estimates, did not show any promise. It has been shown by Sree et al.[4] that, in the case of Poisson sampling, using prefiltering can extend the frequency range up to about three times the mean sampling frequency, or six times the Nyquist frequency, which is amazingly good. However, in the non-Poisson sampling case the frequency range to which reasonable spectral estimates could be made was generally limited to somewhat less than half of the mean sampling frequency, which is just a little less than the Nyquist criterion and, therefore, is not that bad.

Figure 4 shows the normalized spectral estimates of the LV data taken near the shear layer reattachment region in the backward-facing step facility. The spectrum follows the expected shape up to approximately 90 Hz, which is about one-third the mean sampling frequency and two-thirds of the Nyquist criterion. Above that frequency the spectrum appears to be noise. Prefiltering had no effect on the spectral estimates at higher frequencies. The shape of the actual spectrum beyond 90 Hz is quite uncertain in this case. A Poisson process would have revealed the true nature of the spectrum at least up to about the mean sampling frequency and, perhaps, up to about three times that with prefiltering.

Concluding Remarks

Spectral analysis of LV data plays an important role in characterizing a turbulent flow and in estimating the associated turbulence scales, which can be helpful in validating theoretical and numerical turbulence models. The determination of turbulence scales is critically dependent on the accuracy of the spectral estimates. Spectral estimations from "individual realization" LV data are typically based on the assumption of a Poisson sampling process. What this Note has demonstrated is that the sampling distribution must be considered before spectral estimates are used to infer turbulence scales. A non-Poisson sampling process can occur if there is nonhomogeneous distribution of particles in the flow. Based on the study of a simulated first-order spectrum, it has been shown that a non-Poisson sampling process causes the estimated spectrum to deviate significantly from the true spectrum. It is also noted in this case that prefiltering techniques do not improve the spectral estimates at higher frequencies. Further, this Note has addressed only the effect of non-Poisson sampling on the accuracy of the spectral estimates. Effects of other factors such as velocity bias, instrumentation errors, etc. should also be investigated.

Acknowledgment

This research was performed under Research Grant NAG-1-1549 from NASA Langley Research Center, Hampton, Virginia.

References

[1]Srikantaiah, D. V., and Coleman, H. W., "Turbulence Spectra from Individual Realization Laser Velocimetry Data," *Experiments in Fluids*, Vol. 3, No. 1, 1985, pp. 35–44.

[2]Roberts, J. B., and Ajmani, D. B. S., "Spectral Analysis of Randomly Sampled Signals Using a Correlation-Based Slotting Technique," *Institute of Electrical and Electronic Engineers Proceedings*, Vol. 133, Pt. F, No. 2, 1986, pp. 153–162.

[3]Shapiro, H. S., and Silverman, S. A., "Alias-Free Sampling of Random Noise," *Journal of the Society of Industrial Applied Mathematics*, Vol. 8, No. 2, 1960, pp. 225–248.

[4]Sree, D., Kjelgaard, S. O., and Sellers, W. L., III, "On the Measurement of Turbulence Spectra from non-Poisson Sampled Laser Velocimetry Data," AIAA Paper 94-0041, Jan. 1994.

Static Behavior of Laminated Elastic/Piezoelectric Plates

Paul Heyliger*
Colorado State University,
Fort Collins, Colorado 80523

Introduction

EXACT solutions for laminated elastic plates with simple support under transverse load have been developed by Pagano.[1] The resulting displacement and stress distributions demonstrated

Received Oct. 14, 1993; revision received March 23, 1994; accepted for publication April 8, 1994.

*Associate Professor, Department of Civil Engineering.

some of the more severe limitations of classical lamination theory, particularly for thick plates. These results have been extremely useful in assessing the accuracy of numerous laminated plate theories.

Recently, the solution methodology used for elastic plates was extended and applied to laminates composed of piezoelectric layers.[2] Resulting through-thickness distributions of the elastic and electric fields were obtained for several of these laminates under a simple sinusoidal loading or potential. A similar formulation has been applied to a specific case of an intelligent composite by Ray et al.,[3] but this was a specialized case of the present formulation in which, among other assumptions, the piezoelectric coefficient e_{33} was set equal to zero. The formulation in Ref. 3 did not require nor allow for continuity of the electrostatic potential and normal electric displacement at a layer interface.

In this Note, exact solutions are presented for a hybrid laminate containing both piezoelectric and elastic layers under applied surface traction and surface potential. The distributions for displacement, stress, electrostatic potential, and electric displacement are obtained for two different loadings. These results should provide a useful means of comparison in the development of laminated piezoelectric plate theories.

Governing Equations

The geometrical configuration of the laminate is such that the thickness dimension of the laminate coincides with the z direction, with the lengths of the plate in the x and y directions denoted as L_x and L_y, respectively. Each layer of the laminate can be purely elastic, piezoelectric, or conducting. The general problem considered in this study is to determine the behavior of the elastic and electric field components throughout the laminate under an applied mechanical or electrical loading. The forcing function is introduced through either an applied surface displacement, traction, potential, or electric charge. It is also possible to consider internally applied quantities in this formulation.

The class of laminate considered in this study is composed of an arbitrary number of laminae perfectly bonded at their top and bottom surfaces. A single piezoelectric layer has the constitutive equations given by Ref. 4.

$$\begin{aligned} \sigma_{ij} &= C_{ij}S_j - e_{ji}E_j \\ D_i &= e_{ij}S_j + \epsilon_{ij}E_j \end{aligned} \tag{1}$$

Here σ_{ij} are the components of the stress tensor, C_{ij} the elastic stiffness components, S_j the components of infinitesimal strain, e_{ji} the piezoelectric coefficients, E_i the components of the electric field, D_i the components of the electric displacement, and ϵ_{ij} the dielectric constants. Only bidirectional layers are considered in this study, with the poling direction coincident with the x_3 or z axis.

Combining these equations with the field-potential, strain-displacement, and stress strain relations[4] gives the three equilibrium equations $\sigma_{ij,j} = 0$ and the charge equation $D_{i,i} = 0$ in terms of the displacements u, v, and w and the electrostatic potential ϕ as

$$C_{11}u_{,xx} + C_{12}v_{,xy} + C_{13}w_{,xz} + e_{31}\phi_{,xz} + C_{66}(u_{,yy} + v_{,xy}) + C_{55}(u_{,zz} + w_{,xz}) + e_{15}\phi_{,xz} = 0 \tag{2}$$

$$C_{12}u_{,xy} + C_{22}v_{,yy} + C_{23}w_{,yz} + e_{32}\phi_{,yz} + C_{44}(v_{,zz} + w_{,yz}) + C_{66}(u_{,xz} + v_{,xx}) + e_{24}\phi_{,yz} = 0 \tag{3}$$

$$C_{13}u_{,xz} + C_{23}v_{,yz} + C_{33}w_{,zz} + e_{33}\phi_{,zz} + C_{44}(w_{,yy} + v_{,yz}) + C_{55}(u_{,xz} + w_{,xx}) + e_{24}\phi_{,yy} = 0 \tag{4}$$

$$e_{31}u_{,xz} + e_{32}v_{,yz} + e_{33}w_{,zz} + e_{24}(w_{,yy} + v_{,yz}) + e_{15}(u_{,xz} + w_{,xx}) - \epsilon_{11}\phi_{,xx} - \epsilon_{22}\phi_{,yy} - \epsilon_{33}\phi_{,zz} = 0 \tag{5}$$

These represent the governing equations for a single lamina. If the material for a given layer is nonpiezoelectric, the coefficients e_{ij} are zero, and the electric and elastic fields uncouple.

The applied forcing function can be expressed in the form of a Fourier series. For an applied load or potential, each term in such a series can be represented in the form

$$q(x, y) = q_0 \sin px \sin qy \tag{6}$$

$$\hat{\phi}(x, y) = \hat{\phi}_0 \sin px \sin qy \tag{7}$$

where $p = p(m) = m\pi/L_x$ and $q = q(n) = n\pi/L_y$. These expressions can be used for either the top or bottom surface of the laminate.

At each interface between layers, various continuity conditions of must be enforced. These exist for u, v, w, ϕ, σ_z, τ_{xz}, τ_{yz}, and D_z. At a single interface of a laminate with n plies, there are six conditions related to the elastic variables and two conditions related to the electrostatic variables for a total of $8(n-1)$ conditions. At both the top and bottom surfaces, there are three elastic boundary conditions and one electric condition for a total of eight conditions. Enforcing all conditions leads to $8n$ equations relating the variables within all layers of the laminate.

Exact Solution

Solutions for the displacement components and the electrostatic potential are sought in the form

$$\begin{aligned} u(x, y, z) &= U(z)\cos px \sin qy \\ v(x, y, z) &= V(z)\sin px \cos qy \\ w(x, y, z) &= W(z)\sin px \sin qy \\ \phi(x, y, z) &= \Phi(z)\sin px \sin qy \end{aligned} \tag{8}$$

Substitution of these functions into Eqs. (2-5) results in four coupled ordinary differential equations in z, which can be expressed as

$$(C_{11}p^2 + C_{66}q^2)U - C_{55}U'' + pq(C_{12} + C_{66})V - p(C_{13} + C_{55})W' - (e_{31} + e_{15})p\phi' = 0 \tag{9}$$

$$pq(C_{12} + C_{66})U + (C_{66}p^2 + C_{22}q^2)V - C_{44}V'' - q(C_{23} + C_{44})W' - q(e_{32} + e_{24})\phi' = 0 \tag{10}$$

$$p(C_{13} + C_{55})U' + q(C_{23} + C_{44})V' + (C_{55}p^2 + C_{44}q^2)W - C_{33}W'' + (e_{15}p^2 + e_{24}q^2)\phi - e_{33}\phi'' = 0 \tag{11}$$

$$p(e_{15} + e_{31})U' + q(e_{24} + e_{32})V' + (e_{15}p^2 + e_{24}q^2)W - e_{33}W'' - (\epsilon_{11}p^2 + \epsilon_{22}q^2)\phi + \epsilon_{33}\phi'' = 0 \tag{12}$$

A prime denotes differentiation with respect to z. The unknown functions in z are taken in the form

$$\begin{Bmatrix} U(z) \\ V(z) \\ W(z) \\ \Phi(z) \end{Bmatrix} = \begin{Bmatrix} \bar{U} \\ \bar{V} \\ \bar{W} \\ \bar{\Phi} \end{Bmatrix} \exp(sz) \tag{13}$$

Here the overbar denotes a constant, s is an unknown number that is generally complex, and z represents the local coordinate of the given layer. Substitution of these expressions into Eqs. (9–12) yields a system of equations in the roots s. Expressing these equations in matrix form and computing the determinant yields an eighth-order polynomial in even powers of s. The coefficients of this characteristic equation are a function of the plate geometry and material properties of the lamina and can be real, imaginary, or complex. Following computation of these roots, expressions for the displacement and potential functions in Eq. (13) can be obtained, with the stresses and electric displacements determined using the constitutive equations in Eq. (1).

Elastic Layers

The functions describing the distribution of the elastic field components for a nonpiezoelectric layer have been given by Pagano[1] and are not repeated here. These functions are expressed in terms of six unknown constants A_j for a given layer. Since $e_{ij} = 0$ for these layers, the elastic and electric fields uncouple. The electrostatic behavior in this case is represented using the two roots from Eq. (12), or

$$n_{1,2} = \sqrt{\frac{\epsilon_{11}p^2 + \epsilon_{22}q^2}{\epsilon_{33}}} \tag{14}$$

The potential and transverse electric displacement components are given by

$$\phi(x, y, z) = \sin px \sin qy \sum_{j=1}^{2} B_j \exp(n_j z) \tag{15}$$

$$D_z(x, y, z) = -\epsilon_{33} \sin px \sin qy \sum_{j=1}^{2} B_j n_j \exp(n_j z) \tag{16}$$

Hence, the response of the elastic and electric field within the layer is a function of the six constants A_j and the two constants B_j.

Piezoelectric Layers

For some piezoelectric materials, solution of the characteristic equation yields real, imaginary, or complex roots. The solutions corresponding to the real and imaginary roots are given elsewhere[2] and are not repeated here, other than to note that these expressions are typically a function of four constants. The complex values for s^2 appear in conjugate pairs, which result in four roots for s in the form $\pm(a \pm ib)$, where $i = \sqrt{-1}$ and a and b are positive constants. The contribution of the solution for $U(z)$ corresponding to the complex roots in this case can be expressed as

$$U(z) = c_1 e^{az} \cos bz + c_2 e^{az} \sin bz + c_3 e^{-az} \cos bz + c_4 e^{-az} \sin bz \tag{17}$$

where c_1–c_4 are real constants. Following some algebraic manipulations and using Eqs. (9–13), the solution for $V(z)$ can be expressed as

$$V(z) = c_1 e^{az}(\Gamma_1 \cos bz - \Omega_1 \sin bz) + c_2 e^{az}(\Omega_1 \cos bz + \Gamma_1 \sin bz) + c_3 e^{-az}(\Gamma_1 \cos bz + \Omega_1 \sin bz) + c_4 e^{-az} \times (-\Omega_1 \cos bz + \Gamma_1 \sin bz) \tag{18}$$

In all of the remaining expressions, Γ_i and Ω_i are functions of the root s, the material properties, and the loading and geometry of the laminate.[2] The final expression for $W(z)$ can be expressed as

$$W(z) = c_1 e^{az}[(a\Gamma_2 - b\Omega_2)\cos bz + (-b\Gamma_2 - a\Omega_2)\sin bz] + c_2 e^{az}[(b\Gamma_2 + a\Omega_2)\cos bz + (a\Gamma_2 - b\Omega_2)\sin bz] + c_3 e^{-az}[(b\Omega_2 - a\Gamma_2)\cos bz + (-b\Gamma_2 - a\Omega_2)\sin bz] + c_4 e^{-az}[(b\Gamma_2 + a\Omega_2) \times \cos bz + (-a\Gamma_2 + b\Omega_2)\sin bz] \tag{19}$$

A similar expression exists for $\phi(z)$, with the 2 subscript on Γ and Ω replaced by a 3.

The expressions for the stress and electric displacement components can be obtained by the appropriate differentiation and combination with the constitutive equations as given in Eq. (1). For example, the part of the normal stress components corresponding to the complex roots are

$$\begin{aligned}\sigma_{ii} = \big(&c_1 e^{az}\{[-pC_{i1} - qC_{i2}\Gamma_1 + C_{i3}(-2\eta\Omega_2 + \xi\Gamma_2) + e_{3i}(-2\eta\Omega_3 + \xi\Gamma_3)]\cos bz + [qC_{i2}\Omega_1 + C_{i3}(-2\eta\Gamma_2 - \xi\Omega_2) + e_{3i}(-2\eta\Omega_3 + \xi\Gamma_3)] \times \sin bz\} c_2 e^{az}\{[-pC_{i1} - qC_{i2}\Gamma_1 + C_{i3}(\xi\Gamma_2 - \eta\Omega_2) + e_{3i}(\xi\Gamma_3 - \eta\Omega_3)]\sin bz + [qC_{i2}\Omega_1 + C_{i3}(\xi\Omega_2 + \eta\Gamma_2) + e_{3i}(\xi\Gamma_3 - \eta\Omega_3)]\cos bz\} \\ &\times c_3 e^{-az}\{[-pC_{i1} - qC_{i2}\Gamma_1 + C_{i3}(\xi\Gamma_2 - \eta\Omega_2) + e_{3i}(\xi\Gamma_3 - \eta\Omega_3)]\cos bz + [-qC_{i2}\Omega_1 + C_{i3}(\xi\Omega_2 + \eta\Gamma_2) + e_{3i}(\xi\Gamma_3 + \eta\Omega_3)]\sin bz\} \\ &\times c_4 e^{-az}\{[-pC_{i1} - qC_{i2}\Gamma_1 + C_{i3}(\xi\Gamma_2 - \eta\Omega_2) + e_{3i}(\xi\Gamma_3 - \eta\Omega_3)]\sin bz + [qC_{i2}\Omega_1 - C_{i3}(\xi\Omega_2 + \eta\Gamma_2) - e_{3i}(\xi\Gamma_3 + \eta\Omega_3)]\cos bz\}\big)\sin px \sin qy\end{aligned} \tag{20}$$

where $\xi = a^2 - b^2$ and $\eta = 2ab$. The normal component D_z of the electric displacement can be computed using the equation for σ_z by substituting e_{3j} for the C_{j3} and $-\epsilon_{33}$ for e_{33}. There are also terms corresponding to the remaining four roots that must be added to this part of the solution. The remaining components can be calculated with little difficulty.

Solution for the Laminate

The elastic and electric field components within each layer are expressed in terms of eight unknown constants. These are determined using the interface and continuity conditions at the upper and lower surfaces of each lamina. Following the solution of the total system of equations for the constants, the solution for any component can be computed at any location within the laminate.

Numerical Examples

The laminate considered in this example is a [0/90] cross ply composed of an elastic material with piezoelectric layers bonded to the upper and lower surfaces. The plate has side lengths of $L_x = L_y = L$ and the total thickness of h. The elastic layers have thickness of $0.4h$, with the piezoelectric layer thicknesses of $0.1h$. The elastic material is modeled after a fiber-reinforced composite and has the properties $E_{11} = 132.38$ (all in GPa), $E_{22} = 10.756$, $E_{33} = 10.756$, $\nu_{12} = 0.24$, $\nu_{13} = 0.24$, $\nu_{23} = 0.49$, $G_{44} = 3.606$, $G_{55} = 5.654$, $G_{66} = 5.654$, $\epsilon_{11}/\epsilon_0 = 3.5$, and $\epsilon_{22}/\epsilon_0 = \epsilon_{33}/\epsilon_0 = 3.0$. The piezoelectric layers are modeled after PZT-4 and have the material properties $E_{11} = E_{22} = 81.3$ (all in GPa), $E_{33} = 64.5$, $\nu_{12} = 0.329$, $\nu_{13} = \nu_{23} = 0.432$, $G_{44} = G_{55} = 25.6$, $G_{66} = 30.6$, $e_{31} = e_{32} = -5.20$ (all in C/m^2), $e_{33} = 15.08$, $e_{24} = e_{15} = 12.72$,

Table 1 In-plane displacement and potential

	Applied potential		Applied load	
Height	$u \times 10^{12}$	ϕ	$u \times 10^{12}$	ϕ
0.500	−32.764	1.0000	−47.549	0.0000
0.475	−23.349	0.9971	−41.425	0.0189
0.450	−13.973	0.9950	−35.424	0.0358
0.425	−4.6174	0.9936	−29.531	0.0488
0.400	4.7356	0.9929	−23.732	0.0598
0.300	2.9808	0.8415	−10.480	0.0589
0.200	1.7346	0.7014	0.1413	0.0589
0.100	0.8008	0.5707	9.8917	0.0596
0.000	0.0295	0.4476	20.392	0.0611
−0.100	−0.4404	0.3305	24.768	0.0634
−0.200	−0.8815	0.2179	29.110	0.0665
−0.300	−1.3206	0.1081	33.819	0.0706
−0.400	−1.7839	−0.0010	39.309	0.0756
−0.425	−2.0470	−0.0009	44.492	0.0602
−0.450	−2.3140	−0.0008	49.772	0.0425
−0.475	−2.5856	−0.0004	55.163	0.0224
−0.500	−2.8625	0.0000	60.678	0.0000

Table 2 Out-of-plane stresses and electric displacement

	Applied potential		Applied load	
Height	$\sigma_z \times 10^3$	$\sigma_{xz} \times 10^3$	$\sigma_z \times 10^1$	$D_z \times 10^{13}$
0.500	0.0000	0.0000	10.000	160.58
0.475	−0.8333	41.457	9.9657	149.35
0.450	−2.8471	64.626	9.8682	117.23
0.425	−5.3241	69.556	9.7154	66.568
0.400	−7.5482	56.259	9.5151	−0.3382
0.300	−12.957	19.082	8.5199	−0.1276
0.200	−15.245	−4.5693	7.3747	0.0813
0.100	−15.510	−18.203	6.1686	0.2913
0.000	−14.612	−23.866	4.9831	0.5052
−0.100	−12.524	−25.282	3.8045	0.7259
−0.200	−9.2558	−25.633	2.6137	0.9563
−0.300	−5.5018	−24.994	1.4821	1.1995
−0.400	−1.8733	−23.379	0.4868	1.4587
−0.425	−1.1074	−18.888	0.2845	−58.352
−0.450	−0.5162	−13.501	0.1312	−103.66
−0.475	−0.1351	−7.2092	0.0340	−132.40
−0.500	0.0000	0.0000	0.0000	−142.46

Table 3 In-plane stresses

	Applied potential		Applied load	
Height	$\sigma_x \times 10^2$	$\sigma_{xy} \times 10^2$	σ_x	σ_{xy}
0.500	111.81	−146.03	6.5643	−2.4766
0.475	63.736	−100.77	5.8201	−2.1824
0.450	15.833	−55.693	5.0855	−1.8942
0.425	−32.001	−10.698	4.3595	−1.6114
0.400	−79.865	34.295	3.6408	−1.3332
0.400	−51.681	6.3365	2.8855	−0.2463
0.300	−33.135	4.6631	1.4499	−0.1534
0.200	−19.840	3.3247	0.2879	−0.0817
0.100	−9.7737	2.2096	−0.7817	−0.0212
0.000	−1.3905	1.2286	−1.9266	0.0369
0.000	−1.3089	1.2287	0.0991	0.0369
−0.100	−0.5782	0.5227	−0.0149	0.0965
−0.200	0.1348	−0.0572	−0.1280	0.1529
−0.300	0.8463	−0.5840	−0.2426	0.2139
−0.400	1.5723	−1.1220	−0.3616	0.2882
−0.400	14.529	−6.0731	−4.2348	1.5603
−0.425	178.01	−7.3455	−4.8806	1.8105
−0.450	210.98	−8.6346	−5.5337	2.0651
−0.475	244.28	−9.9437	−6.1951	2.3246
−0.500	277.95	−11.276	−6.8658	2.5899

and $\epsilon_{11}/\epsilon_0 = \epsilon_{22}/\epsilon_0 = 1475$, $\epsilon_{33}/\epsilon_0 = 1300$. The piezoelectric layer thicknesses are taken as 0.1 m.

Both applied double sinusoidal loading and surface potentials are considered, with $m = n = 1$ and $q_0 = \phi_0 = 1$. The units of these constants and the resulting elastic and electric field quantities are consistent with those given for the material properties. The aspect ratio in both cases is $L/h = 4$. For the applied load, the top and bottom laminate surfaces are fixed at zero potential. For the applied potential, these surfaces are stress free.

Representative through-thickness distributions are shown in Tables 1–3. The in-plane stress distributions reflect the discontinuous nature at each layer interface. The midplane transverse displacements are -14.711×10^{-12}m for the applied potential and 30.027×10^{-11}m for the applied load.

Closure

The present formulation can be applied to bonded laminates of dissimilar piezoelectric materials, which also require continuity of the eight elastic and electric field variables used here. Embedded piezoelectric layers and specified internal quantities are easily incorporated into the analysis.

References

[1]Pagano, N. J., "Exact Solutions for Rectangular Bidirectional Composites and Sandwich Plates," *Journal of Composite Materials*, Vol. 4, Jan.1970, pp. 20–34.

[2]Heyliger, P. R., "Exact Solutions for Simply-Supported Laminated Piezoelectric Plates," Computational Mechanics Rept. 93-07, Dept. of Civil Engineering, Colorado State Univ., Fort Collins, CO, Aug. 1993.

[3]Ray, M. C., Bhattacharya, R., and Samanta, B., "Exact Solutions for Static Analysis of Intelligent Structures," *AIAA Journal*, Vol. 31, Sept. 1993, pp. 1684–1691.

[4]Tiersten, H. F., 1969, *Linear Piezoelectric Plate Vibrations*, Plenum, New York. Chap. 5.

Dynamic Response of Cross-Ply Shallow Shells with Levy-Type Boundary Conditions

A. A. Khdeir*
Middle East Technical University, 06531 Ankara, Turkey

I. Introduction

THE analysis of laminated composite shells has been the subject of significant research interest in recent years. The classical lamination shell theories based on the Love-Kirchhoff assumptions are adequate to predict the gross behavior of thin laminates. When the structures are rather thick or when they exhibit high anisotropy ratios, the transverse shear deformation effect has to be incorporated. In such cases more refined theories are needed. The third-order theory used in the present study is proposed by Reddy and Liu.[1] Closed-form solutions for the dynamic response of laminated shells have been developed mainly for the case of simply supported boundary conditions. Ritz, Galerkin, and other approximate methods are used for other boundary conditions. The need for analytical solutions for the dynamic response of composite laminates for a variety of boundary conditions is worthy to be mentioned. In the present work, a generalized modal approach in conjunction with the Levy method is presented to solve for the transient response of cross-ply laminated shallow shells with various boundary conditions and for arbitrary loadings. To demonstrate the method, I present numerical results of theories for center deflections of spherical shells subjected to sinusoidal loading in the spatial domain and sine pulse loading in the time domain.

Analytical Solution

A generalized modal approach is used to solve the equations of motion of laminated composite shallow shells with Levy-type boundary conditions. The edges $x_2 = 0, b$ are assumed simply supported, whereas the remaining ones ($x_1 = \pm a/2$) may have arbitrary combinations of free, clamped, and simply supported edge conditions. In this approach, we express the generalized displacements as products of undetermined functions and known trigonometric functions so as to satisfy the simply supported boundary conditions at $x_2 = 0, b$. The equations of motion can be reduced in the following state space equation by defining a state vector $\{y(x_1, t)\}$

$$\{y'\} = [M]\{\ddot{y}\} + [K]\{y\} + \{r\} \tag{1}$$

where a prime and dots on a quantity denote the derivative with respect to x_1 and time t, respectively; $\{r\}$ is the load vector. In the case of a free vibration problem, the vector $\{y\}$ will be separated

Received Oct. 13, 1993; revision received March 7, 1994; accepted for publication March 17, 1994.

*Department of Civil Engineering.